

## Effects of Surface Irregularities and Interfacial Cracks on Polymer Electrolyte Fuel Cell Performance

M. P. Manahan<sup>a</sup>, S. Kim<sup>a,b</sup>, E. C. Kumbur<sup>a,c</sup>, and M. M. Mench<sup>a,\*</sup>

<sup>a</sup> Department of Mechanical and Nuclear Engineering, The Pennsylvania State University,  
University Park, PA 16802, USA

<sup>b</sup> Current affiliation: Pacific Northwest National Laboratory, Richland, WA 99352, USA

<sup>c</sup> Current affiliation: Department of Mechanical Engineering and Mechanics, Drexel University,  
Philadelphia, PA 19104, USA

\* Corresponding author (mmm124@psu.edu)

The present study seeks to investigate the impact of surface irregularities and cracks at the catalyst layer (CL) and micro-porous layer (MPL) interface on the mass and electronic transport of polymer electrolyte fuel cells (PEFCs). Two different CLs were compared, i.e. one with negligible cracking and the other with high cracking (~6% contact surface area reduction), under a combination of various operating conditions, including high/low relative humidity, and the presence of nitrogen/helium inert gases in the cathode inlet stream. A limiting current density analysis indicated that the cracked CL demonstrated a small increase (0.5%) in the Fickian diffusion of the reactants across the cathode electrode compared to the negligible-cracked CL case. Furthermore, the results from a relative humidity analysis showed that the protonic resistance in the CL might dominate the moderate current density region ( $\sim 0.2 \text{ A/cm}^2 < \text{current density} < 0.45 \text{ A/cm}^2$ ). Finally, comparison of the cell performance for cracked and negligible-cracked CL cases suggests that the cracks may act as water pooling sites, which in turn, may enhance the performance in the high current density region ( $\text{current density} > 0.45 \text{ A/cm}^2$ ) due to the decreased water surface coverage and/or enhanced water removal.

### Introduction

Polymer electrolyte fuel cells (PEFCs) maintain the most promising alternative portable energy source, especially for automotive applications. Nonetheless, there still remain substantial areas of research to better understand the dynamics of this complex device and to optimize its components for improved efficiency. Of particular interest is the optimization of the interfaces between the components of a PEFC.

Changes in interfacial morphology of PEFC components can have a significant effect on the cell performance. Several studies [1-6] have investigated the contact resistances and related losses at the bipolar plate and gas diffusion layer interface. In addition, numerous studies have shown that cycling the load and the temperature under normal operating conditions can produce and cause the growth of cracks in the membrane electrode assembly (MEA) [7-9], which may directly affect the morphology of the catalyst layer (CL) micro-porous layer (MPL) interface. In most fuel cell studies, the interface between the CL and the MPL surfaces is assumed to be

perfectly smooth [10,11]; however, in reality, the CL and MPL surfaces are highly rough [12], and therefore the contact between these two layers is not perfect. Recently, several studies have investigated the contact resistance at this interface [13,14]. However, to the best of the authors' knowledge, no studies focused on investigating the effects of surface irregularities at the CL|MPL interface on PEFC performance have been reported. Based on this motivation, this study seeks to understand the impact of surface irregularities and cracks at the CL|MPL interface on PEFC performance by investigating the mass and electronic transport under different operating conditions via a detailed in-situ experimental analysis.

### Experimental

SIGRACET Gas Diffusion Layer™ (SGL 10BB series coated with MPL) and commercially available MEA were used in this study. The CL|MPL interface used in this experimental effort was modified by introducing cracks, effectively reducing the CL contact surface area by approximately 6% (Fig. 1-a). This cracked CL|MPL interface case was compared to the negligible-cracked CL case (Fig. 1-b). The inlet gases used were 5% O<sub>2</sub> with the balance in nitrogen (5%-O<sub>2</sub> nitrox) and 5% O<sub>2</sub> with the balance of helium (5%-O<sub>2</sub> heliox). Two relative humidity conditions were tested, i.e. 100%/100% anode/cathode relative humidity ("wet" conditions) and 70%/50% anode/cathode relative humidity ("dry" conditions), to investigate the effect of liquid water for the cracked and negligible-cracked CL. The inert gases were varied in order to examine the effect of reactant diffusion rate in the cracked versus negligible-cracked CL.

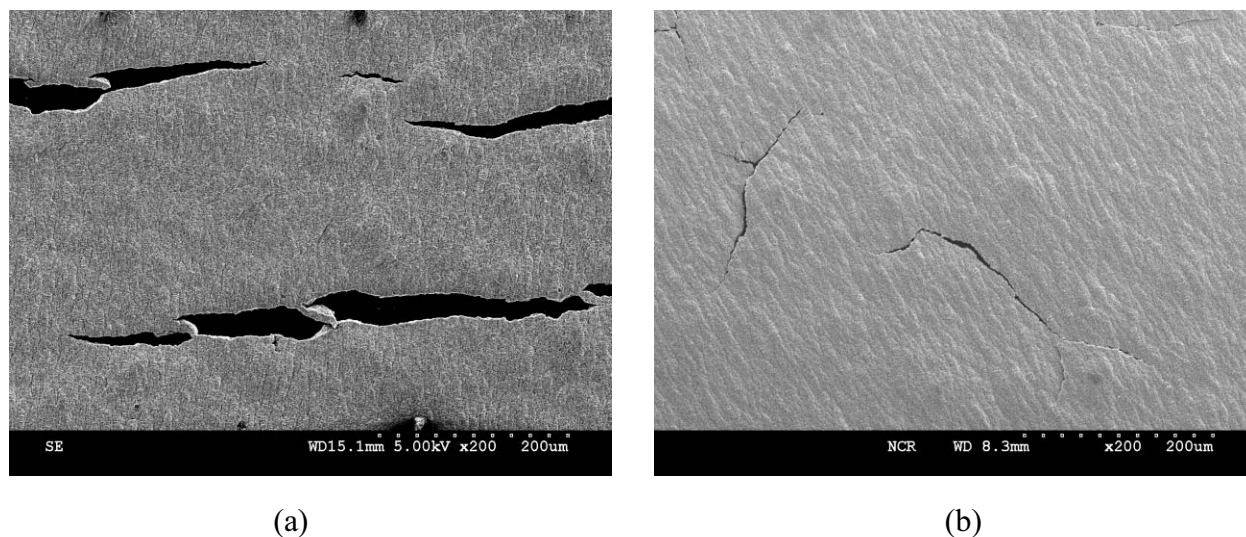


**Figure 1.** SEM images of the surface of the a) cracked CL having crack widths of  $\sim 30\mu\text{m}$ , b) negligible-cracked CL having crack widths of  $\sim 5\mu\text{m}$ .

Typically, variability in cell assembly, component properties, and operating conditions may yield inconsistent/unrepeatable performance data, which may inhibit capturing the effects of surface cracks on the performance. Meticulous care was taken in this study, however, to ensure repeatable data collection in order to reduce experimental uncertainty. Several key tools were employed to eliminate experimental uncertainty, including: *i*) implementation of metallic gaskets to control the overall compression of the components [15,16]; *ii*) use of subgaskets to obtain the

exact MEA active area (area exposed to reactant gases) and double the sealing surface for the silicone gasket (refer to Fig. 3); *iii*) use of silicone gaskets to eliminate the external gas leakage; *iv*) use of coolant to achieve constant temperature boundary conditions and enhance temperature control of cell components [17-19]; and *v*) vertical orientation of gas flow channel design and cell orientation to reduce the amount of buildup of liquid water and minimize the performance variation [20]. Figure 2 illustrates several of the experimental improvements, such as the use of a metallic/silicone gaskets, and precision of the component size/placement.

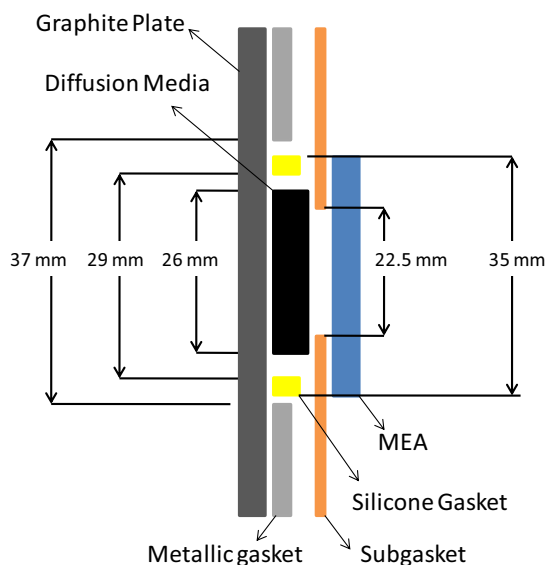


**Figure 2.** A schematic of the cross section of the experimental setup.

Experiments were performed by an in-house fuel cell testing station and an Arbin E-load was used to control the current/voltage cycles. Polarization data for each test were obtained once the cell reached the steady state condition. In each test, the cell was cycled between 0.4 V and OCV conditions for 20 minutes. This step was then followed by 10 minutes of constant 0.6 V operation to ensure that the cell possessed nearly the same water content and temperature distribution regardless of previous testing conditions. Constant current steps were applied and the associated voltage response was monitored. Each constant current step was performed for two minutes in order to achieve steady state condition. Fluctuations in the current density were observed especially in the high current density region. This can be attributed to the flooding conditions and/or oxygen starvation. When the fuel cell could not meet the current draw, a final set of data was taken at 0.1 V constant voltage for 15 seconds in order to measure the limiting current density as accurately as possible without overheating the cell. After one cycle (from zero current to the approximate limiting current), the cell was run at constant 0.6 V for 10 minutes, and then the cycle was repeated two more times.

## Results and discussion

### Effect of Crack on Gas Transport

The first phase of this study was focused on examining the effects of CL surface cracks on the gas transport and evaluating the mode of diffusion (Fickian or other) across the cathode

electrode. A detailed comparison was performed between the limiting current densities of a cracked and a negligible-cracked CL when 5%-O<sub>2</sub> nitrox and 5%-O<sub>2</sub> heliox were used separately in the cathode stream. The ratio of the Fickian (molecular) diffusion coefficient of heliox to nitrox is given [21] as:

$$\left( \frac{D_{O_2-Heliox}}{D_{O_2-Nitrox}} \right)_{\text{numerical}} = 2.8 \quad [1]$$

The limiting current density is defined [22] as,

$$i_l = -nFD_{\text{eff}} \frac{C_{\infty}}{\delta} \quad [2]$$

where  $n$  is the equivalent electrons per mole of reactant,  $F$  is the charge carried on one equivalent mole,  $C_{\infty}$  is the concentration of the reactant at the boundary of the flow channel, and  $\delta$  is the distance to the electrode surface from the flow channel boundary. It was assumed that  $\delta$  and  $C_{\infty}$  are constant because of the efforts made to eliminate the experimental uncertainty in the data collection. Therefore, the ratio of the limiting current density of the 5%-O<sub>2</sub> heliox case and 5%-O<sub>2</sub> nitrox case can be expressed as an experimental ratio of the diffusion coefficients:

$$\frac{i_{l,O_2-Heliox}}{i_{l,O_2-Nitrox}} = \left( \frac{D_{O_2-Heliox}}{D_{O_2-Nitrox}} \right)_{\text{experimental}} \quad [3]$$

The ratio of the limiting current densities noted in Eq. 3 has been determined experimentally and compared to the theoretical Fickian diffusion coefficient ratios given in Eq. 1. Figures 3 and 4 show the polarization behavior of the cell for these two cases, in which the arrow at the high current density region highlights the difference between the limiting current of the 5%-O<sub>2</sub> nitrox and 5%-O<sub>2</sub> heliox. The change in limiting current densities is due to the change in the inert gas from 5%-O<sub>2</sub> nitrox to 5%-O<sub>2</sub> heliox. Table 1 tabulates the experimentally calculated parameters (Eq. 3) divided by the numerical results (Eq. 1) for dry and wet conditions. These results in Table 1 indicate that regardless of moisture content, the percentage of molecular diffusion in the cracked CL was 0.5% higher than that of the negligible-cracked CL, likely resulting from the relatively large voids of the cracks. Furthermore, the percent molecular diffusion of the dry condition cases (both cracked and negligible-cracked CL) was 0.6% higher than the respective wet conditions, indicating that water may fill these voids, forcing more non-Fickian diffusion to occur. In the negligible-crack CL case, the diffusion will tend slightly toward non-Fickian diffusion because of the absence of the larger cracks in the CL. Lower cell temperature testing is currently being conducted in order to ensure liquid water accumulation, which may further exacerbate the differences between the wet and dry conditions for cracked and negligible-cracked CLs.

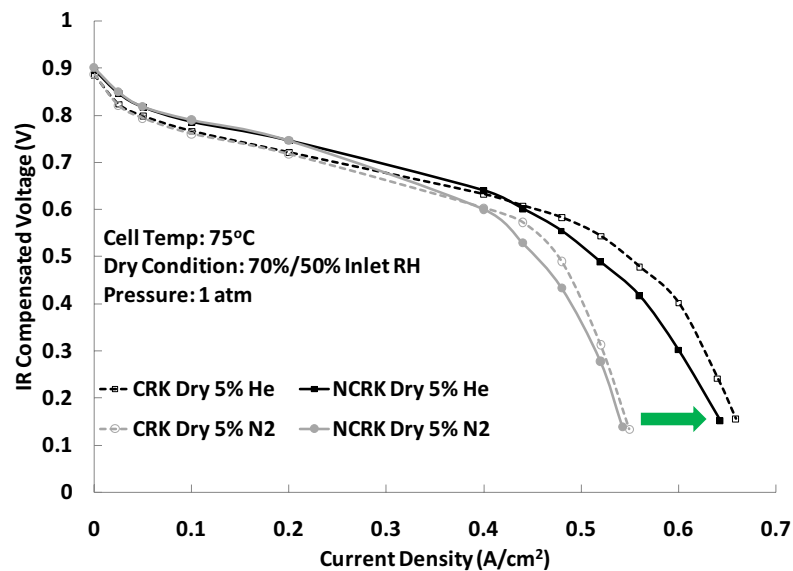


**Figure 3.** A comparison of the experimentally determined limiting current densities of a cracked CL (CRK) and a negligible-cracked CL (NCRK) at dry conditions for 5%-O<sub>2</sub> nitrox (5% N<sub>2</sub>) to 5%-O<sub>2</sub> heliox (5% He).

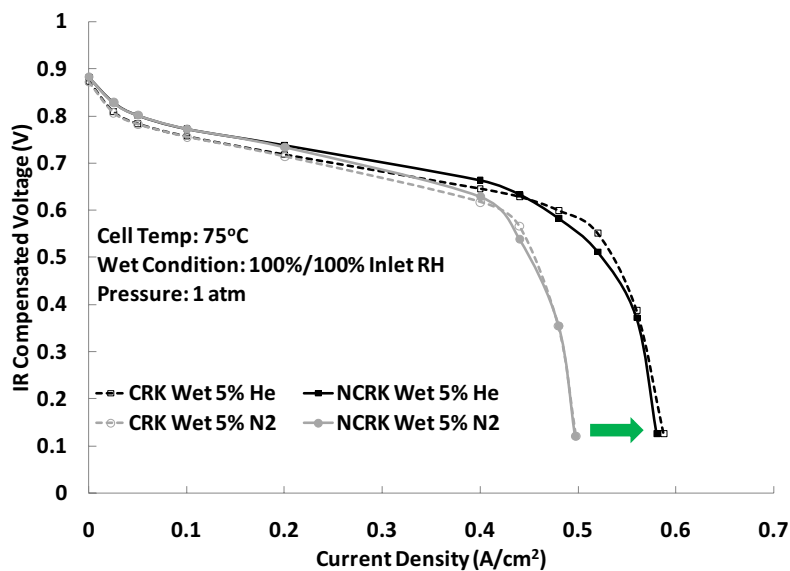


**Figure 4.** A comparison of the experimentally determined limiting current densities of a cracked CL (CRK) and a negligible-cracked CL (NCRK) at wet conditions.

**Table 1.** The experimentally calculated parameters (Eq. 3) divided by the numerical results (Eq. 1) for dry and wet conditions shows the percentage of Fickian diffusion observed.

$\frac{i_{l,O_2-Heliox}}{D_{O_2-Heliox}} \bigg/ \frac{i_{l,O_2-Nitrox}}{D_{O_2-Nitrox}}$	<b>Dry Condition Molecular Diffusion</b>	<b>Wet Condition Molecular Diffusion</b>
Cracked CL	42.8%	42.2%
Negligible-Cracked CL	42.3%	41.7%

### Cracked and Negligible-Cracked CL Performance in Wet and Dry Conditions

The second phase of this study was aimed at investigating the effects of CL surface cracks on the cell performance under wet and dry conditions. Figures 5 and 6 show a comparison of wet and dry conditions for cracked and negligible-cracked CL cases. Based on the experimental data, three distinct regions, as summarized below (also graphically displayed in Figs. 5 and 6), can be indentified for comparing the wet and dry conditions.

- Region I: Dry performance > wet performance
- Region II: Dry performance < wet performance
- Region III: Dry performance > wet performance

Several factors listed in Table 2 can be the cause of these three regions. Depending on the current density, these factors may have varying degrees of relative dominance in the overall performance of the fuel cell. It is important to note that IR-compensated voltage does not account for protonic resistance in the CL, and therefore is not accounted for in Figs. 5 and 6.

**Table 2.** A summary of possible factors involved to explain the behavior of the dry and wet condition performance (Figs. 5 and 6).

<b>Factors affecting cell performance</b>	<b>Dry condition</b>	<b>Comparison</b>	<b>Wet condition</b>
Oxygen diffusion	$D_{O_2,dry}$ (enhanced performance)	>	$D_{O_2,wet}$
Oxygen concentration	$y_{O_2,dry}$ (enhanced performance)	>	$y_{O_2,wet}$
Proton resistance	$R_{H^+,dry}$ (worse performance)	>	$R_{H^+,wet}$
Reaction location	Near membrane	--	Most of CL

Referring to Figs. 5 and 6, in Region I, the reaction may have occurred near the membrane because less active area was necessary to meet the low current draw, making the path of resistance shorter. This may cause the protonic resistance in the CL to be insignificant compared to the oxygen diffusion and/or oxygen concentration amounts, which are higher in dry conditions compared to wet conditions. In Region II, the higher current draw may have forced the entire CL to be utilized, which will increase the relative significance of the protonic resistance compared to the oxygen diffusion or concentration effect. It is important to note that

the start of Region II (where the wet condition began to outperform the dry condition) occurred at a lower current density in the cracked CL case ( $0.2 \text{ A/cm}^2$ ) than in the negligible-cracked CL case ( $0.26 \text{ A/cm}^2$ ). This may occur because the dry condition will naturally tend to have higher protonic resistance (which dominates Region II) and because the presence of cracks may cause the CL to dry out sooner due to the increased access to the CL. Thus, Region II's earlier onset in the cracked CL case supports the theory that protonic resistance may dominate the moderate current density region. Finally, Region III shows that the dry condition displayed enhanced performance over the wet condition. Since oxygen transport may be dominant through the diffusion media and CL, liquid water obstructing the oxygen's path to the reaction site may have caused a decrease in the wet condition performance.

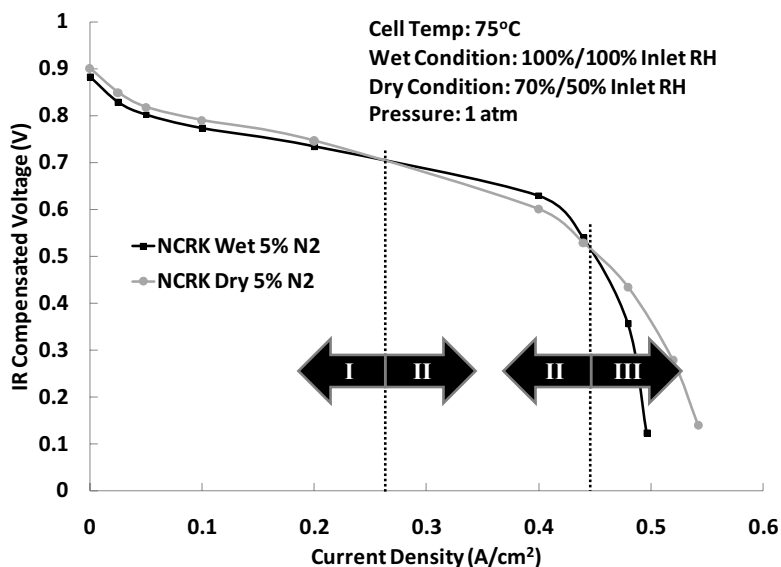


**Figure 5.** A comparison of the polarization curves of wet and dry conditions for negligible-cracked CL (NCRK) cases. The performance was observed to have three distinct regions in which the dry or wet condition outperformed the other. The onset of Region II was observed began at approximately  $0.26 \text{ A/cm}^2$ .

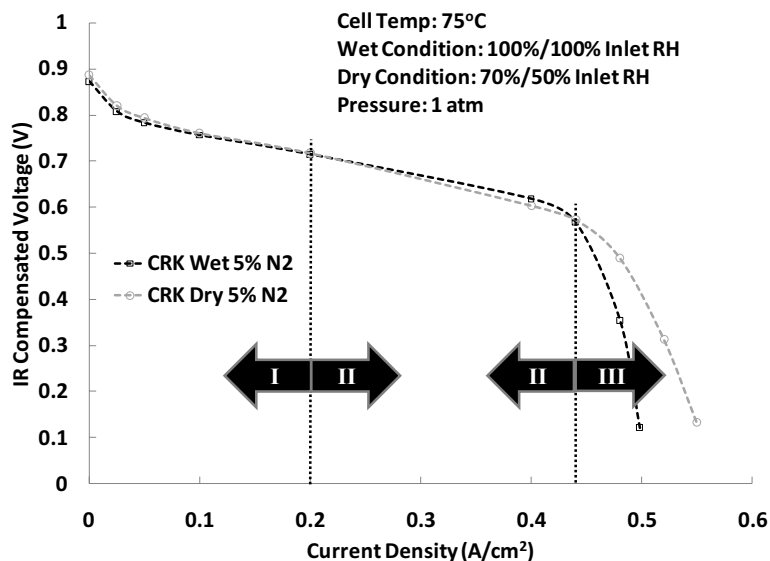


**Figure 6.** A comparison of the polarization curves of wet and dry conditions for cracked CL (CRK) cases. The performance was observed to have three distinct regions in which the dry or wet condition outperformed the other. The onset of Region II began at approximately 0.2 A/cm<sup>2</sup>.

Quantitatively, Table 3 depicts the percentage by which the dry condition outperformed the wet condition. Negative values (Region II) reflect the wet outperforming the dry. Cracks on the CL surface have a significant impact on the performance in Region III, as the improvement between dry and wet conditions for cracked CL is over 16% higher compared to the negligible-cracked CL. This difference between cracked and negligible-cracked CL must be a result of the increase in the performance of the cracked CL in dry conditions because the wet performance is nearly identical for cracked and negligible-cracked CL (Fig. 7). Thus, it might be deduced that the cracks in the CL augment the availability of oxygen transport to the reaction sites in dry conditions. Further investigations are underway to delineate these observations.

**Table 3.** A quantitative summary of the performance of 5%-O<sub>2</sub> nitrox dry condition compared to the wet condition in the three regions for both cracked and negligible-cracked CLs.

Region	Performance Summary	Cracked CL	Negligible-Cracked CL
Region I (0.025 A/cm <sup>2</sup> )	Dry > Wet	1.6%	2.5%
Region II (0.40 A/cm <sup>2</sup> )	Dry < Wet	-2.5%	-4.7%
Region III (0.48 A/cm <sup>2</sup> )	Dry > Wet	38.2%	22.1%

#### Cracked versus Negligible-Cracked CL Performance

The main emphasis in the final phase of this study was placed on the effects that CL surface cracks have on the overall cell performance. This was achieved by comparing the polarization curves of cracked and negligible-cracked CLs at various conditions. Each condition tested showed the same trend as in Fig. 7, where the cracked CL underperformed the negligible-



cracked CL in the lower current density regions by approximately 3%, but the cracked CL performed nearly identically to the negligible-cracked CL in the high current density region (over  $\sim 0.4 \text{ A/cm}^2$ ). The lower performance in the low current density region can be attributed to the reduction in active area due to the cracks. The equal or enhanced performance of the cracked CL to the negligible-cracked CL in the high current density region is possibly due to enhanced water management with a cracked CL, i.e. by reducing a thin film that blocks reactants or by enhancing water removal from the reaction sites. Further investigations are underway to determine the dominating factors involved in this phenomenon.

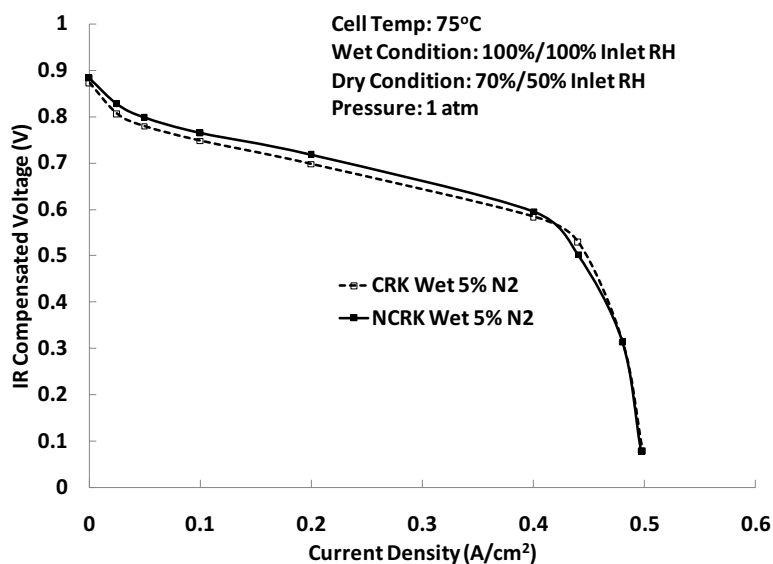


**Figure 7.** A polarization curve comparing a cracked (CRK) and negligible-cracked (NCRK) CL under wet conditions.

### Conclusions

The effects of surface irregularities and CL cracks on the mass and electronic transport of PEFCs were examined by comparing a CL with surface cracks and one with negligible cracking at various operating conditions. It was observed that the presence of cracks on the CL surface yields a slight increase (0.5%) in Fickian diffusion, and that the increase in Fickian diffusion was the same for both wet (100%/100% anode/cathode relative humidity) and dry conditions (70%/50% anode/cathode relative humidity). Further investigations are being conducted to exacerbate the effect of the cracked CL on Fickian and non-Fickian diffusion modes.

Secondly, the performance curves of cracked and negligible-cracked CLs in wet versus dry conditions yielded three distinct regions: *Region I*: low current density regions ( $0 \text{ A/cm}^2 < \text{current density} < \sim 0.2 \text{ A/cm}^2$ ) showed the dry condition outperformed the wet condition by approximately 1.6% in the cracked CL case; *Region II*: the moderate current density region ( $\sim 0.2 \text{ A/cm}^2 < \text{current density} < 0.45 \text{ A/cm}^2$ ) showed the wet condition was up to 2.5% higher voltage than the dry condition for the same cracked CL case; and *Region III*: the high current density region (current density  $> 0.45 \text{ A/cm}^2$ ) showed the dry condition outperformed the wet condition by 38.2% for the cracked CL.

Finally, the presence of cracks on the CL is observed to decrease the performance of the fuel cell by approximately 3% in lower current density region (current density  $< 0.4 \text{ A/cm}^2$ ),

whereas above  $0.4 \text{ A/cm}^2$  the cracked CL performed equal to or better than the negligible-cracked CL even though there is a 6% contact surface area loss due to the cracks. Thus, when the reduced area is accounted for, the cracked CL is outperforming the negligible-cracked CL in the higher current density region, indicating that the cracks may assist with water removal or thin film reduction.

Through this study, it became clear that the presence of surface irregularities may in fact enhance the overall performance at certain operating conditions. Currently, further experiments are being conducted to investigate the several phenomena that will yield further insight regarding the effects of surface irregularities and CL cracks on PEFC performance.

### Acknowledgements

This research was supported by the Toyota Motor Corporation, Japan. M. M. Mench thanks NSF CAREER award #0644811 for partial support.

### References

1. B. Avasarala, P. Haldar, *Journal of Power Sources*, **188**, 225 (2009).
2. Y. Zhou, G. Lin, A.J. Shih, S.J. Hu, *Journal of Power Sources*, **163**, 777 (2007).
3. Z. Wu, Y. Zhou, G. Lin, S. Wang, S. Hu, *Journal of Power Sources*, **182**, 265 (2008).
4. P. Zhou, C. W. Wu, G. Ma, *Journal of Power Sources*, **159**, 1115 (2006).
5. R. Blunk, D. Lisi, Y. Yoo, C. Tucker III, *American Institute of Chemical Engineers*, **49** (1), 18 (2003).
6. A. Kraytsberg, M. Auinat, Y. Ein-Eli, *Journal of Power Sources*, **164**, 697 (2007).
7. W. Liu, K. Ruth, and G. Rusch, *Journal of New Materials for Materials for Electrochemical Systems*, **4**, 227 (2001).
8. Y. Li, J. Quincy, S. Case, M. Ellis, D. Dillard, Y. Lai, M. Budinski, and C. Gittleman, *Journal of Power Sources*, **185**, 374 (2008).
9. Y. Lai, C. Mittelsteadt, C. Gittleman, D. Dillard, *Proceedings of the 3rd International Conference Fuel Cell Science, Engineering, and Technology*, 161 (2005).
10. P. Zhou, C. Wu, *Journal of Power Sources*, **170**, 93 (2007).
11. T. Hottinen, O. Himanen, S. Karvonen, I. Nitta, *Journal of Power Sources*, **171**, 113 (2007).
12. F. Hizir, T. Swamy, S. Ural, E. Kumbur, M. Mench, *Proceedings of the 7th International Conference on Fuel Cell Science Engineering and Technology, American Society of Mechanical Engineers*, 85092 (2009), in press.
13. I. Nitta, O. Himanen, M. Mikkola, *Electrochemistry Communications*, **10**, 47 (2008).
14. R. Makharia, M. Mathias, D. Baker, *Journal of the Electrochemical Society*, **152** (5), A970 (2005).
15. J. Ge, A. Higier, H. Liu, *Journal of Power Sources*, **159**, 922 (2006).
16. I. Nitta, T. Hottinen, O. Himanen, M. Mikkola, *Journal of Power Sources*, **171**, 26 (2007).
17. A. Weber and J. Newman, *Journal of the Electrochemical Society*, **153** (12), A2205 (2006).
18. M. Coppo, N. Siegel, M. von Spakovsky, *Journal of Power Sources*, **159**, 560 (2006).
19. L. Wang, A. Husar, T. Zhou, H. Liu, *International Journal of Hydrogen Energy*, **28**, 1263 (2003).
20. A. Mughal; X. Li, *International Journal of Environmental Studies*, **63** (4), 377 (2006).
21. Toyota Motor Company Internal Communication (2009).
22. M. Mench, *Fuel Cell Engines*, p. 219, John Wiley & Sons, Hoboken (2008).